JOURNAL OF GEOPHYSICAL RESEARCH, VOL. 100, NO. C9, PAGES 18,393–18,408, SEPTEMBER 15, 1995

Equatorial wave sequence associated with warm pool displacements during the 1986–1989 El Niño–La Niña

Joël Picaut and Thierry Delcroix

Groupe SURTROPAC, L'Institut Français de Recherche Scientifique pour le Développement en Coopération (ORSTOM), Nouméa, New Caledonia

Abstract. In the Pacific equatorial band the zonal displacement of the eastern edge of the warm pool, subject to insignificant seasonal variations, is dominated by strong interannual variations almost in phase with the Southern Oscillation Index. Over the 1971–1973 El Niño–La Niña period, Gill (1983) suggested that such displacement was caused solely by horizontal advection by zonal current anomaly. Basin-wide Geosat-derived zonal surface current anomalies are available during the 1986–1989 period, and they agree quite well with observed equatorial currents in the western and central Pacific. Within the 4°N–4°S equatorial band the cumulative contribution of first-baroclinic Kelvin and first-symmetric ($m = 1$) Rossby modes to surface zonal equatorial current anomalies account for most of the Geosat-derived current variability. From these Geosat-derived currents it is demonstrated that the eastward (westward) displacement of the eastern edge of the warm pool was primarily due to horizontal advection by zonal current anomalies during the 1986–1987 El Niño (1988–1989 La Niña). As a corollary, the El Niño (La Niña) warm (cold) sea surface temperature (SST) anomaly in the central western Pacific was the result of anomalous zonal advection. The 1986–1989 displacement of the warm pool appeared as a low-frequency movement resulting from high-frequency forcing, i.e., a succession of local wind forcing and its remote Kelvin and $m = 1$ Rossby wave responses in the equatorial waveguide. In the central western Pacific a $m = 1$ downwelling Rossby wave, issued from the eastern Pacific, shifted the displacement from eastward to westward and therefore seems to have been the cause for El Niño to turn to La Niña in boreal fall 1987. In the eastern Pacific the simultaneous occurrence of free-propagating downwelling (upwelling) Kelvin waves with the seasonal SST warming (cooling) appeared necessary for the development of local El Niño (La Niña) SST anomaly. Over most of the equatorial Pacific, slow migration of SST anomalies clearly showed up, distinct during El Niño and La Niña. These zonal migrations appeared to result from the delayed association of two phenomena: the zonal advection in the central western Pacific and the arrival of downwelling (upwelling) Kelvin waves into the eastern Pacific, synchronous with the seasonal SST warming (cooling). Albeit different in terms of equatorial wave action, as compared to the delayed action oscillator theory, our results suggest that zonal advection and wave dynamics were both important for the generation and migration of El Niño–Southern Oscillation SST anomalies in 1986–1989. Finally, our observational results about warm pool displacements, equatorial wave sequence, the shift from El Niño to La Niña, and the slow SST migrations are presented in a schematic form involving sequential ocean-atmosphere coupling which appears continuously over the November 1986 to February 1989 period.

1. Introduction

In a series of seminal papers, *Bjerknes* [1969, 1972] suggested a link between an interannual atmospheric standing wave, known as the Southern Oscillation (SO), and an anomalous sea surface temperature (SST) warming in the tropical Pacific Ocean, known as El Niño. At the surface the SO results in a pressure seesaw between the southeastern tropical Pacific and the north of Australia (Southern Oscillation Index (SOI), Figure 1). When the SOI is negative (positive), there is usually a westerly (easterly) surface wind anomaly in the western central Pacific, and the surface water is warmer (colder) than normal in the eastern central tropical Pacific. This corresponds to a coupled system in which surface wind anomalies cause and, in turn, are caused by SST changes. The warm phase of the interannual oceanic oscillation has long been known as El Niño, and only recently has the cold phase been studied and named anti-El Niño or La Niña [*Philander*, 1985]. As a consequence, the El Niño–Southern Oscillation (ENSO) acronym is now used to characterize the ocean-atmosphere coupled system connecting El Niño, La Niña, and the SO.

Owing to its most devastating effects [e.g., *Canby*, 1984], El Niño has been studied more extensively than its counterpart La Niña. El Niño appears as an eastward transfer of warm water from the western to the eastern Pacific, and *Wyrtki* [1975] was the first to suggest that the appearance of warm water in the eastern Pacific results from westerly wind anomalies in the central western Pacific, which generate equatorial downwelling

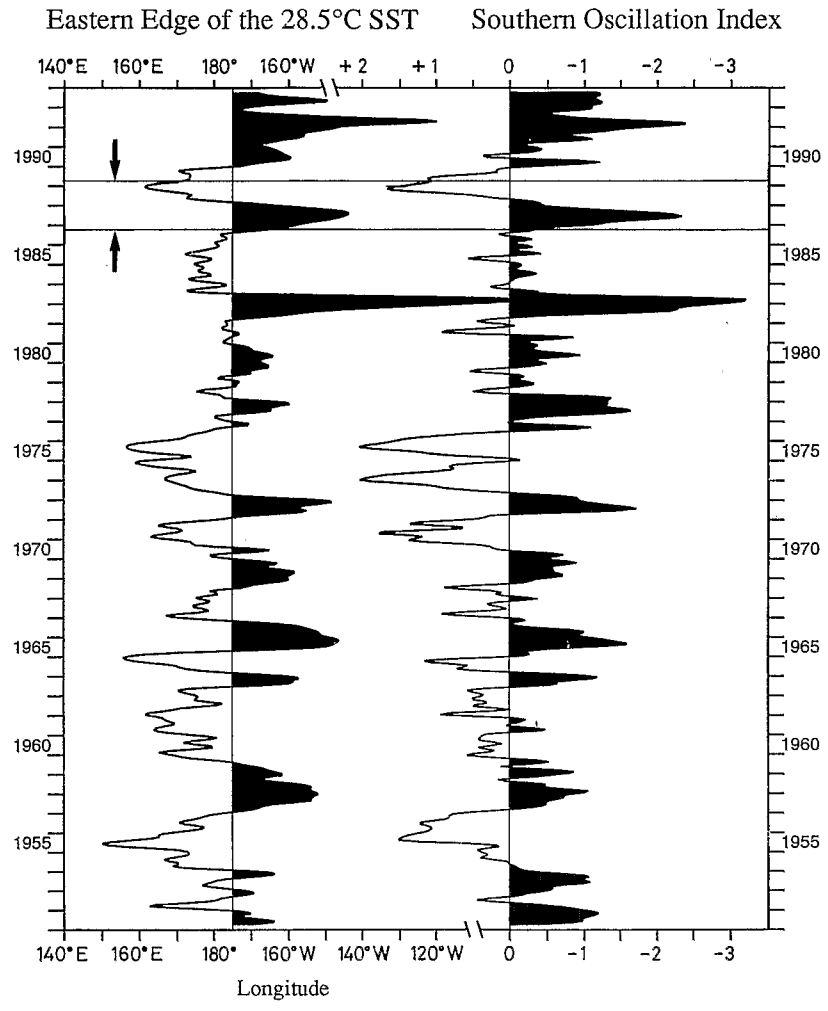

Figure 1. Zonal displacement of the (left) 28.5°C sea surface temperature (SST) averaged over 4°N–4°S and (right) Southern Oscillation Index (SOI) from 1950 to 1993. Monthly values are smoothed with a 1-2-1 filter, and the SOI axis is inverted. The November 1986 to February 1989 period of study is outlined within the two arrows.

Kelvin waves. The importance of Kelvin waves in setting up El Niño is now acknowledged [e.g., *McCreary*, 1976; *Busalacchi et al.*, 1983; *Miller et al.*, 1988]. The corresponding El Niño warming in the eastern Pacific results mainly from the deepening of the thermocline, inhibition of the mean upwelling, and eastward advection of warm water from the west [*Philander*, 1981; *Gill*, 1983; *Harrison and Schopf*, 1984]. Conversely, the cooling associated with La Niña in the eastern tropical Pacific is likely due to westward advection of cold water from the coast of South America and to the increase of upwelling that result from easterly wind anomalies in the central western Pacific and associated remote upwelling Kelvin waves.

The western tropical Pacific is characterized by surface water warmer than 28–29°C (the warm pool). During El Niño the warm pool spreads into the central Pacific and exceptionally into the eastern Pacific [*Gill and Rasmusson*, 1983]. The opposite phenomenon occurs during La Niña, with cold water entering the warm pool region [*Delcroix et al.*, 1992]. As shown in Figure 1 and discussed by *Lukas and Webster* [1992], in the equatorial band, the zonal displacement of the eastern edge of the warm pool is dominated by strong interannual variations (standard deviation of 18.1° longitude) almost in phase with the SOI. Interestingly, the displacement exhibits an insignificant seasonal signal (standard deviation of 1.5° longitude), in contrast to other El Niño–La Niña indices such as SST in the eastern Pacific. The present study will focus upon such displacement during the 1986–1989 El Niño and La Niña cycle. To set the context, Figure 2 represents the mean SST fields during the boreal summers of 1986, 1987, and 1988. Despite a weak warming in the central Pacific [*McPhaden and Hayes*, 1990] the summer of 1986 can be used to illustrate a phase close to "normal." At that time the eastern equatorial Pacific upwelling was near its typical seasonal maximum (July–September), and the warm pool position and SOI were close to their mean positions (Figure 1). One year later, El Niño was fully developed, with a very weak seasonal equatorial upwelling in the eastern Pacific and a warm pool that had moved eastward by about 25° longitude near the equator. By summer 1988, La Niña conditions had almost reached their maxima, with an equatorial upwelling well developed as far as 165°E and a warm pool pushed toward the western Pacific boundary.

Using the linear equatorial-wave theory, *Gill* [1983] first suggested that the zonal displacements of the warm pool and hence the temperature variations in the central Pacific are due to anomalous advection of warm water. He found that the anomalous advection in 1972–1973 resulted from anomalous

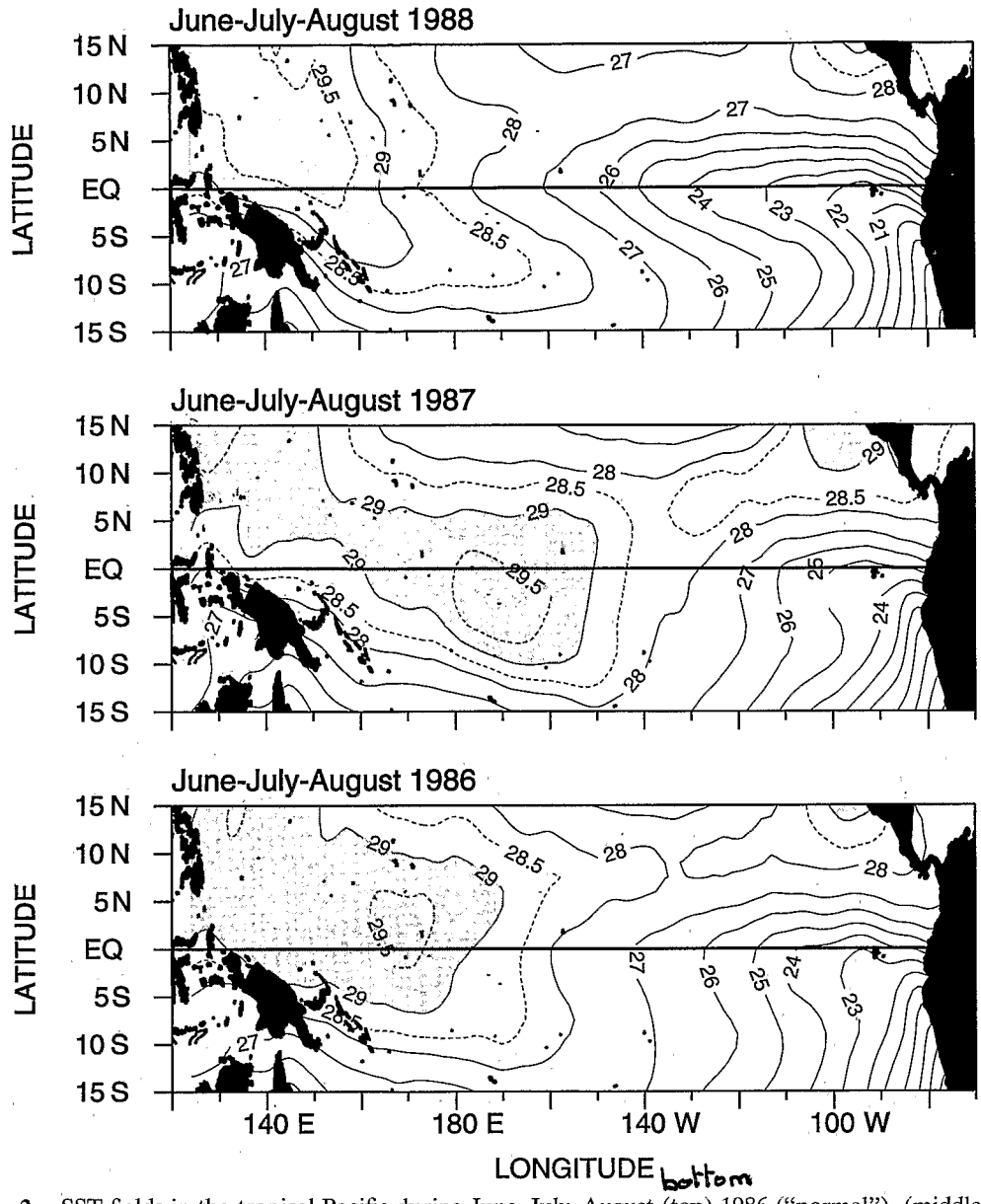

Figure 2. SST fields in the tropical Pacific during June–July–August (top) 1986 ("normal"), (middle) 1987 (El Niño), and (bottom) 1988 (La Niña). Contour interval is 1°C, except for the 28.5 and 29.5°C isotherms. SST warmer than 29°C is shaded.

local wind forcing and mostly from its remote response through a succession of equatorial Kelvin and low-order meridional Rossby waves. *McPhaden and Picaut* [1990] reinforced this idea through direct velocity measurement at 165°E in 1986–1988 and intuited the role of an equatorial Rossby wave. *Delcroix et al.* [1992], through the analysis of 21 oceanographic cruises along the same meridian, clearly showed the importance of wind forcing and of a series of equatorial Kelvin and Rossby waves in the depletion and filling up of the warm pool during the 1986–1988 El Niño–La Niña cycle. Through modeling studies, various authors [*Battisti*, 1988; *Seager*, 1989; *Harrison and Graig*, 1993] have estimated the balance of the terms in the ocean thermodynamic equation and suggested that horizontal advection was important in warming the central Pacific during El Niño. Vertical advection associated with downwelling Kelvin waves may also be important in warming the eastern Pacific. The waves depress the thermocline and reduce the cooling from the deep layer associated with the mean upwelling. The downward heat flux is no more balanced by the cooling from below, and this results in warmer SST. However, contributions from other processes, such as zonal and meridional advection and vertical mixing, cannot be dismissed [*Hayes et al.*, 1991a].

During a strong El Niño, as in 1982–1983, zonal advection may result in a slow eastward displacement of anomalous SST all the way to the eastern Pacific [*Gill and Rasmusson*, 1983]. On the other hand, a more typical El Niño starts with warm SST anomalies near the northern coast of South America that expand slowly westward into the eastern equatorial Pacific [*Rasmusson and Carpenter*, 1982]. Recently, these slow "propagative" SST anomalies have been at the core of research for the understanding of ENSO [e.g., *Anderson and McCreary*,

1985; *Neelin*, 1990]. The slow SST mode, as defined by *Neelin* [1991], is contrasted with the delayed action oscillator mechanism [*Schopf and Suarez*, 1988; *Battisti*, 1988; *Cane*, 1992]. The slow SST mode involves unstable basin-wide coupled ocean-atmosphere modes, and equatorial oceanic waves are unimportant. The delayed action oscillator involves local air-sea interaction in the central eastern part of the basin, and equatorial oceanic waves are essential; it is through the repetitive action of equatorial upwelling Kelvin waves, issued from the reflection of equatorial upwelling Rossby waves, that El Niño ends and then shifts to La Niña.

The delayed action oscillator mechanism involves oceanic equatorial waves which have long been thought difficult to discern individually [*Philander et al.*, 1992]. Such waves are sometime hidden by local forcing, periodic forcing, and multiwave reflections, if not dissipated by mean currents [*Chang and Philander*, 1989; *Rothstein et al.*, 1988]. With the recent deployment of the Tropical Ocean and Global Atmosphere–Tropical Atmosphere Ocean (TOGA-TAO) array of moorings in the equatorial Pacific [*Hayes et al.*, 1991b] and the launch of Geosat and TOPEX/POSEIDON satellites, it is now possible to unambiguously observe these equatorial waves [e.g., *Miller et al.*, 1988; *Busalacchi et al.*, 1994]. More important, these observations enable us to assess the role of equatorial waves in the equatorial transfer of mass and heat [*Delcroix et al.*, 1991] and in the slow eastward migration of the warm pool [*Kessler et al.*, 1995] during El Niño.

Following a careful analysis of Geosat-derived surface currents [*Delcroix et al.*, 1994], the present study shows the importance of a series of first-baroclinic equatorial Kelvin and first-meridional mode Rossby waves in the eastward advection of the warm pool toward the central Pacific and its withdrawal during the successive El Niño and La Niña of 1986–1989. Most of all, it establishes zonal advection through anomalous current as the dominant cause of SST anomalies in the central western Pacific during the 1986–1989 ENSO cycle. A schematic representation of this ENSO cycle is proposed, which suggests some sequential coupling between the SST and wind anomalies which appears continuously over the November 1986 to February 1989 period. The importance of a set of equatorial downwelling Rossby waves in the shift from El Niño to La Niña is discussed, together with the slow westward and eastward progression of SST anomalies during the successive 1986–1989 El Niño–La Niña. The importance of the timing of the wave sequence with regard to the mean seasonal cycle is presented. Finally, all these results are discussed in view of other ENSO events, some recent uncoupled and coupled model results, and the latest ENSO theories.

2. Data and Processing

The bulk of this analysis relies upon a recent version of the Geosat Geophysical Data Records (GDR) which uses improved satellite orbit and water vapor corrections [*Cheney et al.*, 1991]. The way we have processed these GDR to obtain gridded fields of sea level anomalies, surface current anomalies, and the relative contribution of Kelvin and Rossby modes is only outlined here; details are given by *Delcroix et al.* [1994].

The first step of the GDR processing was to retrieve sea surface heights, covering the tropical Pacific from November 1986 to February 1989, using all environmental corrections given in the GDR. Second, along each track we "removed" the geoid and the mean sea surface topography in computing sea level anomalies (SLA) relative to the 2-year period from November 8, 1986, to November 7, 1988 (i.e., the first 43 17-day repeat cycles of the Geosat Exact Repeat Mission). Third, 200-km (total length) nonlinear median and linear Hanning filters were applied to the along-track SLA, following the technique discussed by *Picaut et al.* [1990]. Fourth, we minimized residual orbit error through the removal of a first-order polynomial trend along each 35°S–35°N track. The next step of our processing was to summarize the irregularly distributed SLA onto a regular 0.5° latitude, 5° longitude, and 5-day grid. Finally, the gridded SLA were smoothed with 3.5° latitude, 15° longitude, and 35-day Hanning filters to reduce remaining small-scale noise.

Meridional derivatives of SLA were used to derive low-frequency surface geostrophic zonal current anomalies. The first derivative was used off the equator. At the equator, where geostrophy has long been debated since the work of *Jerlov* [1953], the second derivative yields reliable low-frequency zonal currents as shown and discussed by *Picaut et al.* [1989, 1990]. An equatorially trapped correction factor was added to SLA in order to ensure the continuity between the first and second derivatives of SLA; this specific technique is detailed by *Picaut and Tournier* [1991]. This resulted in a gridded field of surface geostrophic zonal current anomalies (ZCA) in the tropical Pacific. One should remember that each parameter of the processing (along-track and time/space filter lengths, orbit correction scheme, meridional grid size in the first- and second-order derivatives, etc.) was adjusted so that Geosat-derived zonal current anomalies best fit near-surface zonal currents measured at three equatorial moorings at 165°E, 140°W, and 110°W. In contrast to a classical gridding procedure of Geosat data, this adjustment technique provides the most stringent test of the use of altimeter observations to estimate sea level and surface current, given the sensitivity of equatorial geostrophic current to small sea level variations. Owing to the "removal" of the geoid and mean sea surface topography, one must keep in mind that all the results of the present paper are relative to averages computed over the November 8, 1986, to November 7, 1988, period. This 2-year reference period covers two complete seasonal cycles, together with one warm and one cold interannual event (El Niño and La Niña) of similar amplitude, so as to minimize possible seasonal and interannual biases and to approach a climatological mean. Given the results of *Delcroix et al.* [1991] based on a 13-month reference period, the choice of reference is apparently nonessential for the following analyses on equatorial waves.

Multiple comparisons between Geosat-derived sea level and surface current anomalies versus in situ observations are presented by *Delcroix et al.* [1994]. As an example, Figure 3 shows a comparison between Geosat-derived sea level anomalies and 0/500-dbar dynamic height anomalies derived from the TOGA-TAO mooring at 0°–140°W. The correlation coefficient between the two time series is 0.91, with a rms difference of 5.1 cm. Figure 3 clearly stresses that sea level variations reflect the inphase vertical displacement of the first 300-m isotherms (in fact, down to the lowest 500-m TAO sensor) and, in particular, the thermocline displacement (i.e., the 20°C isotherm). Figure 4 shows comparisons between Geosat-derived surface current anomalies and the directly measured near-surface current anomalies at the equator and 165°E, 140°W, and 110°W. The correlation coefficients between Geosat-derived currents versus the measured currents are 0.92, 0.70, and 0.49 from west to east, with corresponding rms differences of 17, 24, and 31 cm

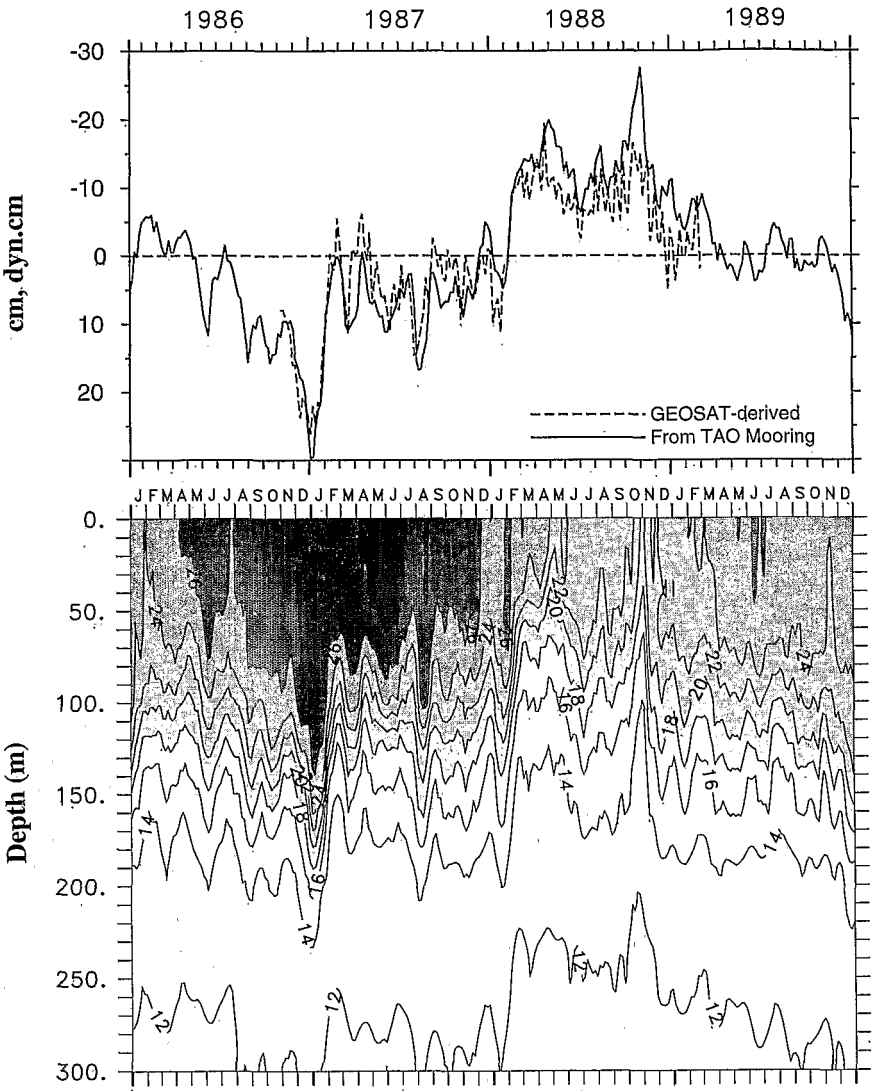

Figure 3. (top) Comparison between Geosat-derived sea level and 0/500-dbar dynamic height anomalies at 0–140°W (relative to November 1986 to October 1988). The vertical axis is inverted so sea level corresponds to isotherm displacement. (bottom) Isotherm depth distribution within 0–300 m at 0°–140°W; contour interval, every 2°C. All data are 5-day averaged to better identify individual equatorial waves.

s^{-1}. Note that the mean measured currents over the 2-year reference period are small, i.e., −2, −14, and −17 cm s^{-1} at 165°E, 140°W, and 110°W, respectively. Of most interest for the present study over the 1986–1989 period, the low-frequency variations of zonal surface currents can be fairly well deduced from Geosat data within a region (165°E–140°W) encompassing the western and eastern limits of the displacement of the eastern edge of the warm pool (Figure 5). In the eastern Pacific the poor agreement between Geosat-derived and observed current (r = 0.49 at 0°–110°W) is probably linked to insufficient density of the surrounding Geosat data, to dynamical reasons [*Delcroix et al.*, 1994], and to inadequate tidal corrections [*Busalacchi et al.*, 1994].

Applying the theoretical approach developed by *Cane and Sarachik* [1976, 1981] to the aforementioned Geosat-derived sea level and surface current fields, *Delcroix et al.* [1994] demonstrated that the first-baroclinic Kelvin and first-symmetric (m = 1) Rossby modes account for 71% of the total variance in ZCA within 4°N–4°S. In order to interpret the zonal displacement of the eastern edge of the warm pool near the equator, we will therefore concentrate upon the relative contribution of these two modes to ZCA. As a consequence, it must be kept in mind that these two modes, which are maximum at the equator in terms of current, reproduce quite well the current variability within 4°N–4°S (see also section 3.1 and Figure 5).

Additional data will be used in the following sections. They include SST and Florida State University (FSU) pseudo wind stress fields, both available on a monthly basis and on a 2° latitude by 2° longitude grid [*Reynolds*, 1988; *Goldenberg and O'Brien*, 1981]. For consistency with the Geosat-derived current processing the SST and FSU fields have been calculated relative to the November 1986–October 1988 reference period and smoothed with a 14° longitude Hanning filter. Note that only zonal wind stress in the equatorial waveguide will be used since we will discuss long equatorial Kelvin and m = 1 Rossby waves.

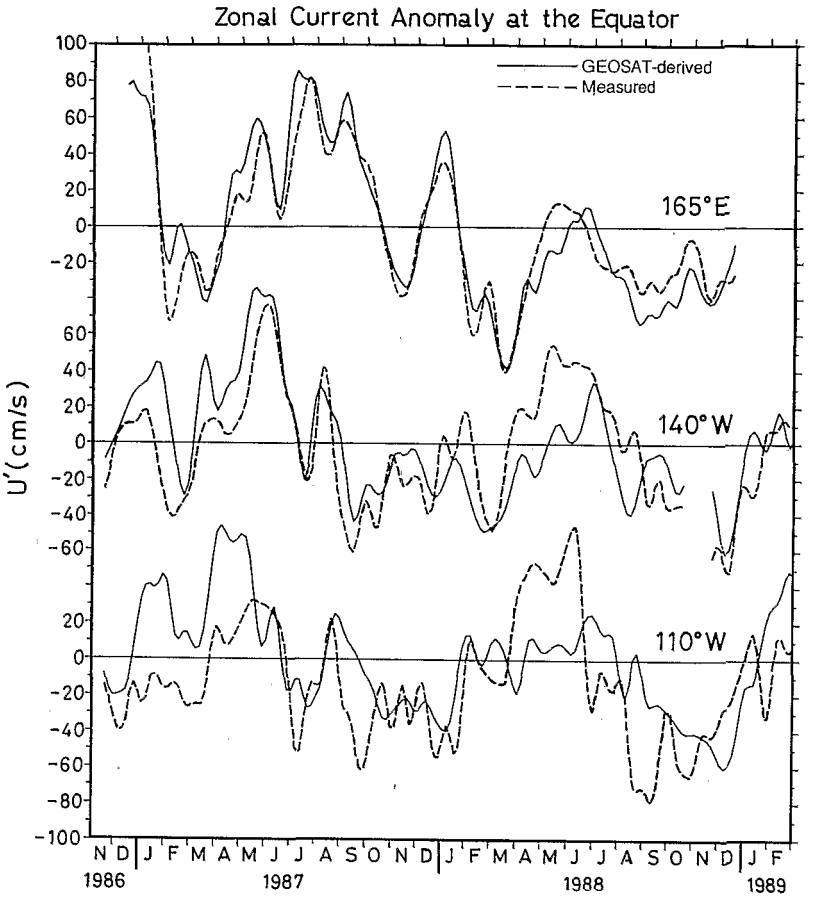

Figure 4. Comparison between Geosat-derived zonal surface current anomaly and near-surface measured current anomaly at the equator and (top) 165°E, (middle) 140°W, and (bottom) 110°W. Positive current anomaly is eastward, and units are centimeters per second [from *Delcroix et al.*, 1994].

3. Displacement of the Warm Pool and Wave Sequence

3.1. Zonal Advection in the Central Western Equatorial Pacific

Figure 5 represents the longitude/time variations of SST averaged over the 4°N–4°S equatorial band. The latitudinal extent of this band was chosen because zonal currents and SST anomalies (SST anomaly normalized by the standard deviation of SST) are greater there than anywhere in the tropical Pacific [*Delcroix et al.*, 1994; *Harrison*, 1989]. The eastern equatorial Pacific is characterized by a pronounced seasonal cycle with SST minima in August–September and SST maxima in March–April. This typical SST seasonal cycle was strongly modulated by the El Niño and La Niña episodes, with water warmer than normal in February–April 1987 and water colder than normal in July–November 1988 (Figure 5). In contrast to the eastern equatorial Pacific, the western equatorial Pacific does not exhibit any SST seasonal cycle [*Delcroix*, 1993]. The El Niño and La Niña episodes appeared through an eastward expansion of the warm pool in 1987 followed by its shrinking in 1988. Specifically, using the 28.5°C isotherm as the eastern edge of the warm pool, we noted an eastward migration of the warm pool from 160°W to 140°W over the November 1986 to July 1987 period, followed by a continuous westward displacement from 140°W to 165°E over the August 1987 to October 1988 period. A quick look at Figure 6 indicates that these zonal displacements may result from a period of notable eastward flow anomalies during El Niño, followed by westward flow anomalies during La Niña. Eastward and westward phase propagation is also evident in Figure 6, suggesting Kelvin and Rossby wave propagation.

Following *Gill*'s [1983] results, we estimated the displacement of water particles transported by the anomalous zonal currents shown in Figure 6. In other words, we calculated the trajectories of two hypothetical drifters transported by the 4°N–4°S averaged ZCA. These trajectories are represented by the thick solid lines in Figures 5 and 6. The hypothetical drifters were launched at 165°E and 180° at the end of November 1986. A sensitivity study on these trajectories was performed in two ways. First, we used the sum of the Kelvin and $m = 1$ Rossby contribution to ZCA (thick dashed lines in Figures 5 and 6) instead of the complete ZCA (thick solid lines in Figures 5 and 6). The excellent agreement between the thick dashed and thick solid lines clearly shows that the Kelvin and $m = 1$ Rossby contributions are sufficient to account for the ⟨4°N–4°S⟩ trajectories. A second test was done, using different boundaries for the latitudinal average. A 2°N–2°S (6°N–6°S) average results in an increase (decrease) of the maximum zonal displacement of the drifters in mid-1987 by about 10° longitude as compared to the ⟨4°N–4°S⟩ displacement. However, the shape of the trajectories remains unchanged, with the return of the drifters in the western Pacific almost at the same

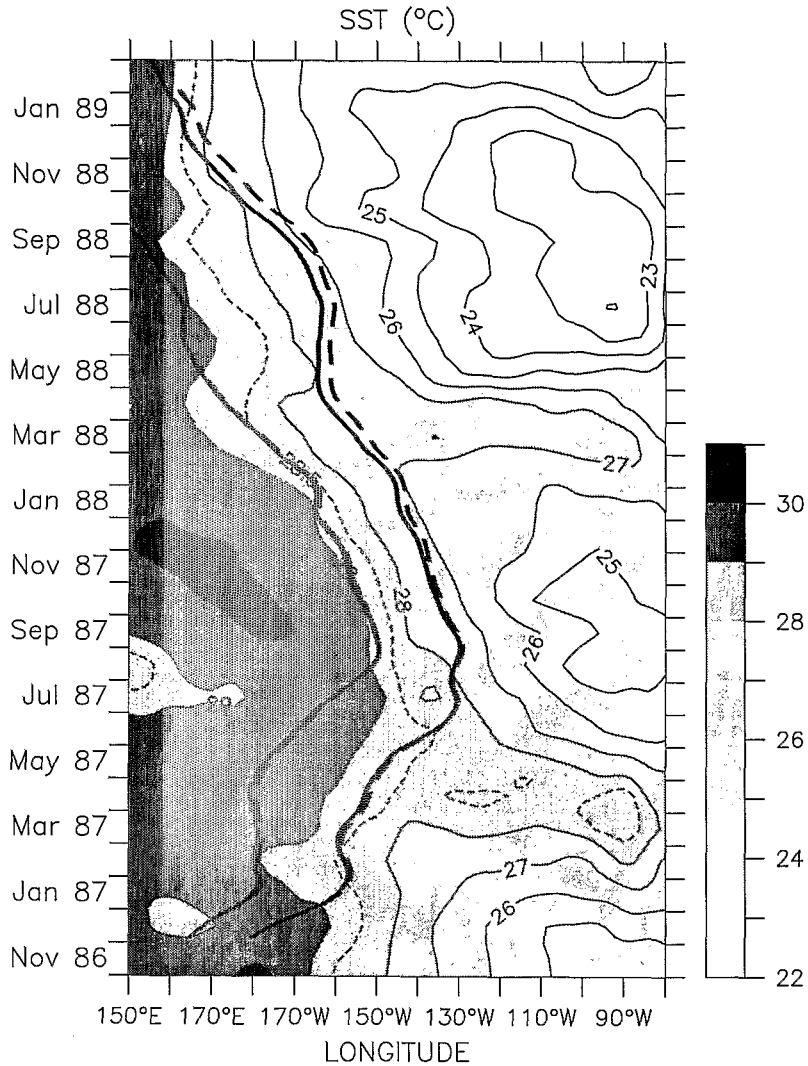

Figure 5. Longitude-time distribution of 4°N–4°S averaged SST. Contour interval is 1°C, except for the 28.5°C isotherm. Superimposed as thick lines are the trajectories of two hypothetical drifters moved by 4°N–4°S averaged surface current anomalies derived from Geosat data (thick solid lines correspond to the total currents; thick dashed lines to the Kelvin and $m = 1$ Rossby mode contributions).

location and time by the end of 1988. These changes due to averaging over different equatorial bands are also quantitatively discussed in the last paragraph of section 3.1.

From Figure 5 there is a predilection for the two trajectories to bracket the 28.5°C isotherm over the considered time period. In addition, there are some hints that small-scale displacements may be common to the 28.5°C displacement and the trajectories (e.g., around January–April 1987 and March–July 1988). Assuming a constant zonal SST gradient ($\partial T/\partial x$) within the two trajectories (looking at Figure 5, this assumption is reasonable within the 28.5–29°C isotherms), the good fit between the 28.5°C isotherm and the trajectories reflects the dominance of anomalous zonal currents in changing SST. A more convincing test is to check the importance of zonal advection in the equation governing the equation of heat within the two trajectories; in this domain the Lagrangian derivative of SST is close to zero since the trajectories bracket the 28.5°C isotherm

$$\partial T/\partial t + u\partial T/\partial x + v\partial T/\partial y + w\partial T/\partial z = 0 \qquad (1)$$

Leaving the discussion to the first two terms for the moment (we will demonstrate a posteriori that these account for most of the variance), where $u = u' + U$ (anomalous and mean zonal currents, respectively), (1) simplifies to

$$\partial T/\partial t = -u'\partial T/\partial x - U\partial T/\partial x \qquad (2)$$

The comparison of the first two terms of (2), averaged between the two trajectories, is shown in Figure 7 (to prevent possible confusion between Lagrangian and Eulerian approaches, note that these two terms were calculated at each grid point (x, t) of Figures 5 and 6 and then averaged between the two trajectories). Given the error remaining in the SST data [*Reynolds*, 1988], a 1-2-1 filter was applied to the two curves of Figure 7 in order to reduce the noise resulting from the derivative in time and space. With the removal of the geoid the mean (November 1986 to October 1988) zonal current U cannot be derived from Geosat data, preventing the calculation of the third term in (2). However, the 4°N–4°S averaged U can be roughly estimated using mean near-surface current values interpolated between

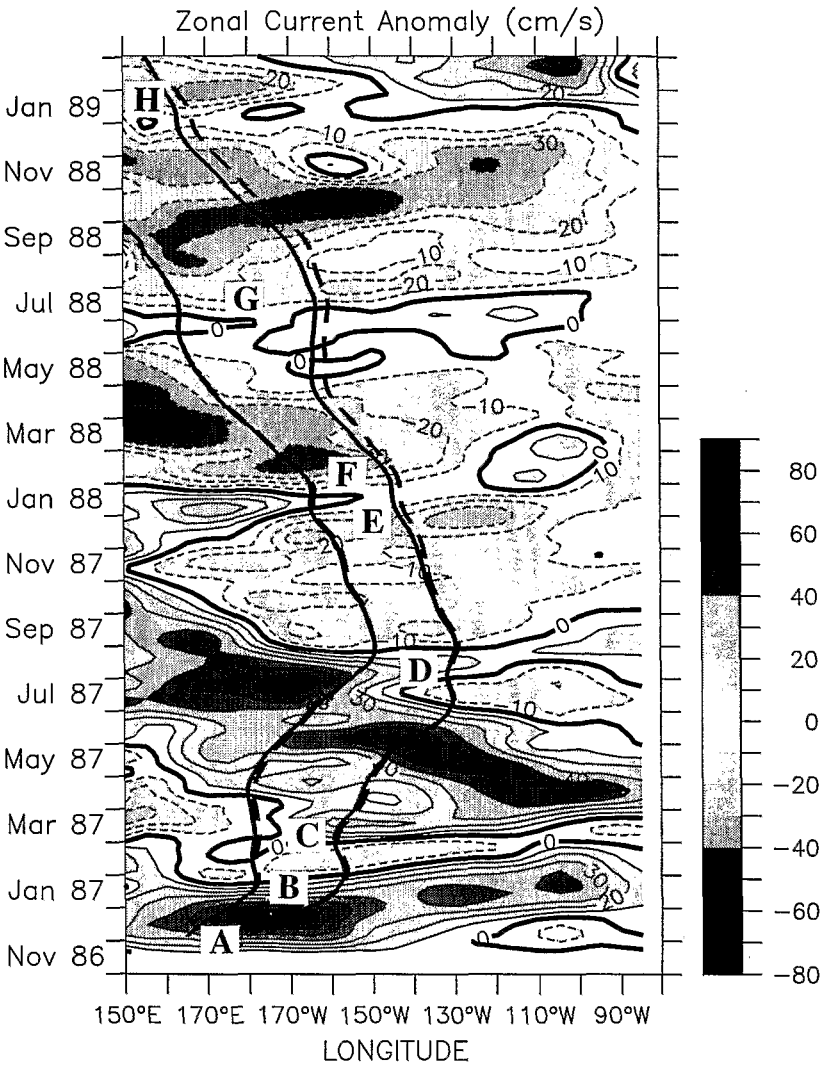

Figure 6. Longitude-time distribution of 4°N–4°S averaged surface current anomaly derived from Geosat. Contour interval is 10 cm s^{-1}. Solid (dashed) lines denote eastward (westward) current anomalies. Thick solid and thick dashed lines are as in Figure 5. Letters A–H denote major zonal current changes within the trajectories, as discussed in section 3.2.

the 0°–165°E (−2 cm s^{-1}) and 0°–140°W (−14 cm s^{-1}) mooring data (Figure 4), multiplied by a 0.75 factor which accounts for the mean ratio between currents averaged over 4°N–4°S and currents at the equator (factor estimated from *Delcroix et al.* [1994, Figure 5]). As expected from the small values of the mean currents (~−5 cm s^{-1}) compared to the time-varying currents (Figures 4 and 6), the use of this estimate of U does not improve the balance of terms in (2), as the rms differences between SST tendency and advective terms remain of the same order (0.16 and 0.13°C/month with and without $-U\partial T/\partial x$).

The curves in Figure 7 present very similar behaviors, with two main oscillations of equivalent amplitude and a ratio of standard deviations (first term over second term of (2)) very close to unity (0.97). This ratio increases (decreases) to 1.30 (0.74) when the two terms of (2) are calculated over 6°N–6°S (2°N–2°S) instead of 4°N–4°S and justifies a posteriori the 4°N–4°S choice. In the eastern Pacific, anomalous advection cannot be rigorously quantified since the Geosat-derived currents u' inadequately compared to observations at 0°–110°W (Figure 4). However, an estimate of (2) indicates that the first two terms do not balance, with, in particular, a ratio of their standard deviations 5–8 times greater than in the central western Pacific. In any case, the fit between the two curves of Figure 7 is relatively good, given the noise remaining in the Geosat-derived current and SST fields; it confirms that zonal advection by anomalous currents is a dominant mechanism for SST variations in the central western equatorial Pacific during the 1986–1989 El Niño–La Niña period.

3.2. Wave Sequence

Plates 1a and 1b show the 4°N–4°S averaged contributions of the first-baroclinic Kelvin and $m = 1$ Rossby modes in ZCA. As discussed above, these two modes represent most of the zonal equatorial current variability and account for the zonal advection of the eastern edge of the warm pool during the 1986–1989 El Niño–La Niña period. A general description of the course of these equatorial horizontal modes and their possible relationship with the wind forcing is presented by *Delcroix et al.* [1994]. In this section we discuss the wave sequence that appears responsible for the displacement of the

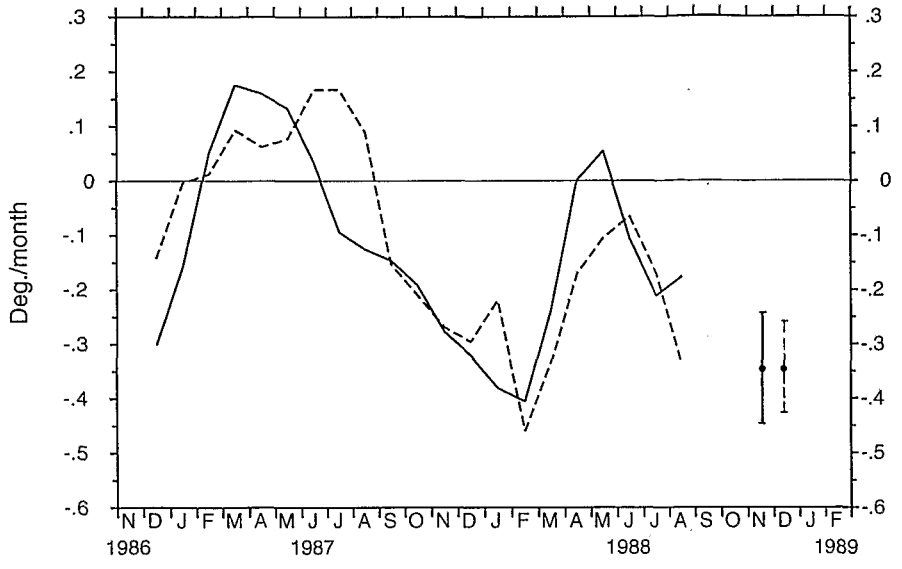

Figure 7. Comparison between SST tendency ($\partial T/\partial t$, solid line) and zonal advection of temperature ($-u'\partial T/\partial x$, dashed line) calculated in between the two trajectories of Figures 5 and 6. The 4°N–4°S averages are only computed up until August 1988, when one trajectory goes beyond the western limit of our current field. An estimation of the mean standard errors of $\partial T/\partial t$ and $-u'\partial T/\partial x$ is represented in the bottom right corner.

eastern edge of the warm pool and its possible role in the central and eastern equatorial SST and vertical thermal structure. For this purpose, we also consider the zonal wind stress and SST anomalies (Plates 1c and 1d) averaged over the 4°N–4°S band and the vertical thermal structure at 0°–140°W (Figure 3). Overall, there are some similarities between Plates 1c and 1d and Figure 6, with nearly simultaneous warm (cold) SST anomalies, westerly (easterly) wind stress anomalies, and eastward (westward) ZCA during El Niño (La Niña).

The Kelvin and $m = 1$ Rossby contributions to the ZCA fields (Plates 1a and 1b) represent a combination of free and wind-forced waves of the system and possible residuals resulting from the fact that we are using a linear physic in the mathematical mode decomposition. However, a lag-correlation analysis done for each of these two fields results in mean phase speeds of 3.1 and 1.1 m s^{-1}, respectively [*Delcroix et al.*, 1994] and suggests that many of the "wave" structures evidenced in Plates 1a and 1b propagate freely at the theoretical speed of the first-baroclinic mode. The course of the wave sequence in ZCA and related parameters is presented, following the time progression of the trajectories of the hypothetical drifters and their main changes, as indicated by labels A to H in Figure 6 and Plate 1. From A to E the relationship between wind forcing and waves was analyzed by *du Penhoat et al.* [1992], who compared sea level anomalies from an ocean linear model, forced by FSU wind stress, with Geosat over the first half (November 1986 to November 1987) of our period of study.

Change A–B (November 1986 to January 1987). The significant eastward displacement was induced by the local response to the strong November–December 1986 westerly wind anomaly centered at 175°E, together with its remote response in the way of a well-defined downwelling Kelvin wave ($u' > 0$) [*Miller et al.*, 1988; *Delcroix et al.*, 1991]. The downwelling Kelvin wave reached the central eastern Pacific in January 1987 and depressed the thermocline by 50 m (Figure 3), acting against the mean equatorial upwelling. Moreover, the arrival of this wave in the eastern Pacific corresponded to the beginning of warm SST anomaly in phase with the regular February–April seasonal warming. According to *du Penhoat et al.* [1992], the reflection of the Kelvin wave on the eastern boundary was canceled by unfavorable westerly wind anomalies in the central and eastern Pacific around March–April 1987 (Plate 1c).

Change B–C (February 1987). The tiny westward displacement was the result of the local and remote response to an easterly wind anomaly all along the equator that generated a small upwelling Kelvin wave ($u' < 0$). This wave, more easily discernible on Figure 3 than on Plate 1a, propagated all the way to the eastern Pacific in agreement with the results of *du Penhoat et al.* [1992].

Change C–D (March–August 1987). The eastward displacement was induced by the cumulative effects of several phenomena: the local response to the westerly wind anomaly in the central Pacific (~150°W), an upwelling Rossby wave ($u' > 0$), and a series of downwelling Kelvin waves. The upwelling Rossby wave, also discernible in Figure 3, was generated around March–April 1987 in the central eastern Pacific by the westerly wind anomaly, which extended all the way from the western to the eastern Pacific. According to the model results of *du Penhoat et al.* [1992], this Rossby wave was enhanced by the eastern boundary reflection of the February–March 1987 upwelling Kelvin wave. The greatest downwelling Kelvin wave was forced in July 1987 around 160°W by the westerly wind anomaly and resulted in a 30-m thermocline depression at 0°–140°W (Figure 3).

Change D–E (August–December 1987). The shift from eastward to westward displacement was due to a downwelling Rossby wave ($u' < 0$) propagating at least from 100°W (July 1987) to at least 160°E (November 1987). This Rossby wave started in the eastern Pacific in a period of favorable easterly wind anomaly, yet model results suggest that the Rossby wave was mostly issued from the reflection of a downwelling Kelvin

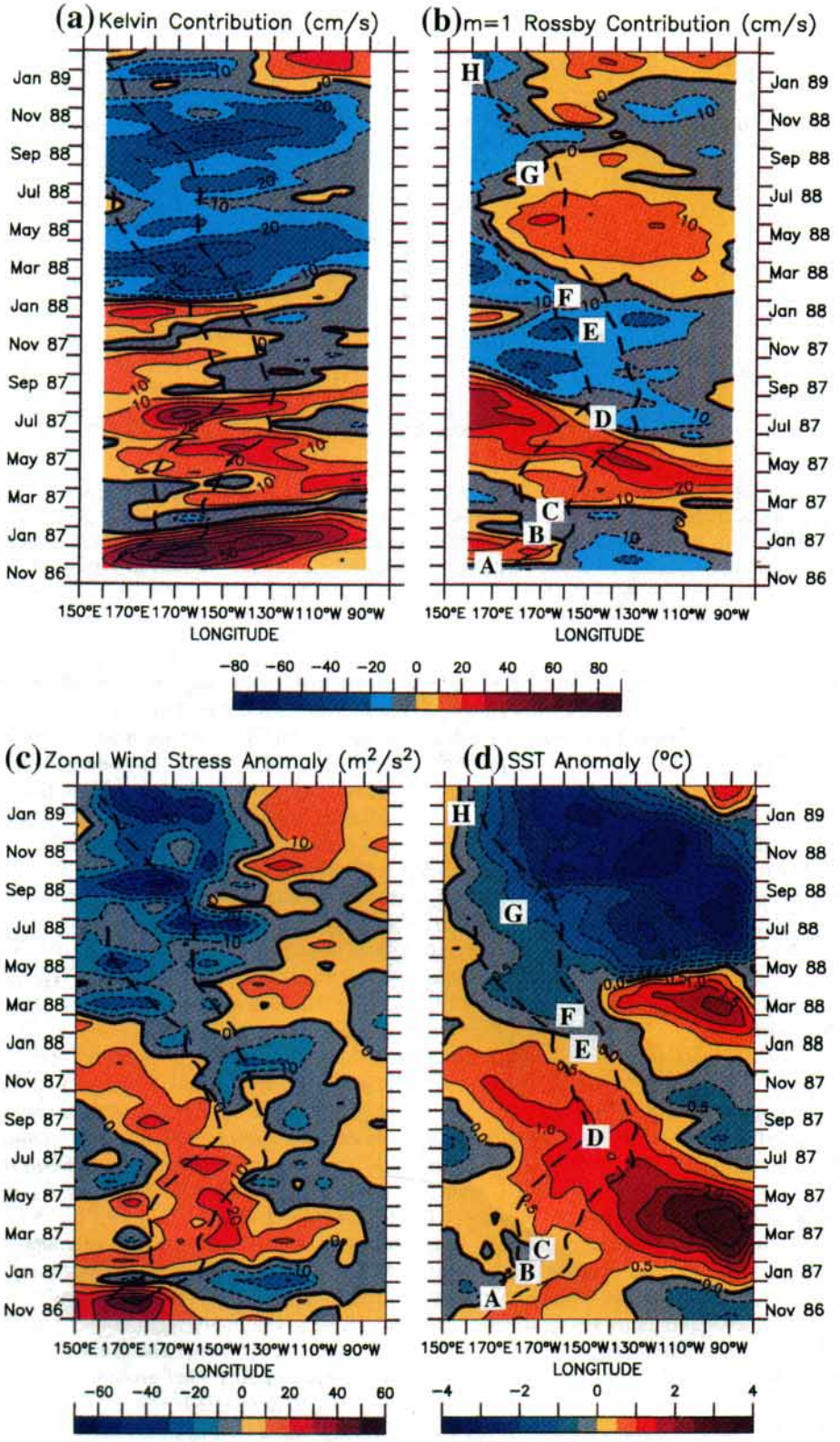

Plate 1. Longitude-time distributions of 4°N–4°S averaged surface current anomalies derived from Geosat data projected onto (a) first-baroclinic Kelvin and (b) $m = 1$ Rossby modes, (c) pseudo zonal wind stress anomalies, and (d) SST anomalies. Contour intervals are 10 cm s^{-1} in Plates 1a and 1b, 10 m^2 s^{-2} in Plate 1c, 0.5°C in Plate 1d. Solid (dashed) lines denote eastward (westward) current anomalies in Plates 1a and 1b, westerly (easterly) wind stress anomalies in Plate 1c, and warm (cold) SST anomalies in Plate 1d. Thick dashed lines and letters A–H are same as in Figure 6.

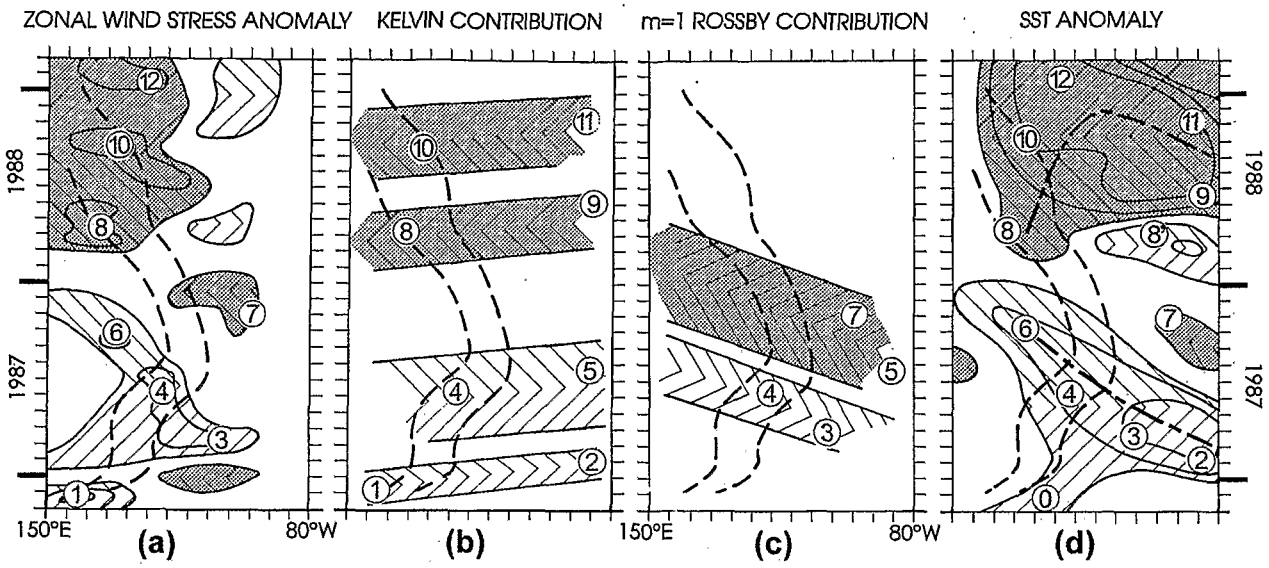

Figure 8. Schematic of the 1986–1989 El Niño–La Niña ocean-atmosphere coupled system, with (a) pseudo zonal wind stress anomaly, (b) Kelvin wave zonal current contribution, (c) $m = 1$ Rossby wave zonal current contribution, and (d) SST anomaly. The open hatched areas and shaded hatched areas denote positive and negative anomalies, respectively. Thick dashed lines correspond to the trajectories of the two hypothetical drifters. Thick dot-dashed lines in Figure 8d indicate apparent SST propagation, as discussed in section 3.3.

wave on the eastern boundary in April 1987 [cf. *du Penhoat et al.*, 1992, Figures 2, 3, and 7]. This westward displacement was maintained later on by the September–December 1987 easterly wind anomaly in the central eastern Pacific, together with its downwelling Rossby wave response.

Change E–F (January 1988). The westward displacement briefly stopped. The current associated with the previously cited downwelling Rossby wave counteracted the current corresponding to a well-defined downwelling Kelvin wave (also clearly detectable at 0°–140°W with a 30-m deepening of the thermocline; see Figure 3). This Kelvin wave may have been forced by the westward extension of the westerly wind anomaly into the western Pacific and/or may have resulted from the reflection of the downwelling Rossby wave arriving on the western boundary in November–December 1987 [*Delcroix et al.*, 1994].

Change F–G (February–July 1988). The continuation of the westward displacement resulted from the combination of local easterly wind anomaly forcing and the dominance of the westward current associated with an upwelling Kelvin wave over the eastward current associated with an upwelling Rossby wave. The upwelling Kelvin wave was most probably generated around March 1988 by an easterly wind anomaly in the western Pacific (~170°E). The upwelling Rossby wave seemed to be forced by a westerly wind anomaly in the eastern Pacific (~130°W) around April 1988. The upwelling Kelvin wave, also apparent at 0°–140°W with a 30-m uplift of the thermocline (Figure 3), arrived in the eastern Pacific in May 1988 and apparently reinforced the buildup of the seasonal cooling.

Change G–H (August 1988 to January 1989). The westward displacement accelerated, mostly due to the local response to a series of easterly wind anomalies, with the strongest in September 1988 around the date line. The September 1988 easterly wind anomaly likely generated a well-defined upwelling Kelvin wave, which resulted in the surfacing of the thermocline at 0°–140°W (Figure 3), and contributed to the enhancement of the seasonal upwelling in the eastern Pacific.

3.3. Schematic Representation and Tentative Explanations

This section is an attempt to present in schematic form the development of the 1986–1989 ENSO coupled ocean-atmosphere system in view of the major phenomena that emerge from the preceding chronological presentation. In addition to section 3.1 that quantitatively established the importance of zonal advection in the displacement of the warm pool, this section presents some conceptual ideas on the development of the 1986–1989 ENSO, with special emphasis on the displacement of the warm pool. In particular, it is assumed that the response of the wind to SST anomalies (and vice versa) occurs on a short timescale [*Gill*, 1985] and therefore can happen in specific areas rather than across the whole basin. Hereafter, the systematic use of cause and effect (e.g., wind generates equatorial waves, waves alter SST, SST modifies wind) should thus be considered with caution, as more data analyses supported by specific modeling studies (uncoupled and coupled) would be necessary to prove or disprove this schematic view of the ENSO cycle in 1986–1989. Nevertheless, we believe the admittedly crude scheme presented in this section to be instructive, as small observational studies are performed to unravel ENSO mechanisms. Figure 8 presents a simplified version of Plate 1 with its general patterns retained for absolute values greater than 10 $m^2 s^{-2}$ for zonal wind stress anomalies (Figure 8a), 15 cm s^{-1} for Kelvin and Rossby wave contributions to ZCA (Figures 8b and 8c), and 0.5°C for SST anomalies (Figure 8d), all relative to the November 1986 to October 1988 reference period. In the following discussion the common numbers encircled in Figure 8 identify what we think to be the major interrelated phenomena (in time and space), e.g., a1 refers to the encircled 1 in Figure 8a, b5 to the 5 in Figure 8b, etc.

By the end of November 1986, El Niño had already started (d0) from possible downwelling Kelvin wave effects (see section 4), but the major onset came from the westerly wind anomaly in the western Pacific (a1). This anomaly moved the

warm pool eastward and generated a downwelling Kelvin wave (b1). This wave arrived in the eastern Pacific in January–February 1987 (b2), depressed the thermocline by 50 m on its passage (Figure 3), and enhanced the regular seasonal SST warming (Figure 5). The resulting warm SST anomaly (d2 and d3) gave rise to a notable development of El Niño in the eastern Pacific and induced a westerly wind anomaly in the eastern Pacific (a3) in March 1987. This westerly anomaly generated an upwelling Rossby wave (c3) propagating all the way to the western Pacific. Both local wind-forced and wave-induced advection sustained the eastward displacement of the warm pool up until August 1987. This eastward displacement into the central Pacific resulted in warm SST anomalies in the central Pacific around July 1987 (d4) and then in the western Pacific around October 1987 (d6). These SST anomalies apparently expanded the westerly wind anomalies farther west (a4 and a6).

Back to April 1987, in the central Pacific the westerly wind anomaly (a4), likely caused by warm SST anomaly (d4), generated downwelling Kelvin waves (b4). These waves, on their way to the coast of South America, contributed to the development of positive SST anomalies in the central Pacific through advection of warm water from the west and depression of the thermocline (Figure 3). At the coast (b5) these Kelvin waves reflected as downwelling Rossby waves (c5) according to *du Penhoat et al.* [1992]. These Rossby waves were reinforced by an easterly wind anomaly (c7 and a7), probably related to the seasonal SST cooling in the eastern Pacific during August–September 1987 (d7), obviously reduced by El Niño (Figure 5). The set of Rossby waves (c5 and c7) shifted the displacement of the warm pool from eastward to westward. With the return of the lending edge of the warm pool from the central to the western Pacific, a cold SST anomaly started to develop in the central western Pacific in February–April 1988 (d8). At the same time (d8') a warm SST anomaly was present in the eastern Pacific; its duration, zonal extension, and magnitude (Plate 1d) corresponded to a normal seasonal SST warming, as compared to non-La Niña or non-El Niño February–April seasonal warming such as in 1986, 1989, and 1990 (all relative to our November 1986 to October 1988 reference period). Therefore the cold SST anomaly in the central western Pacific (d8) was the very first manifestation of La Niña on SST over the whole equatorial Pacific, and the downwelling Rossby waves (c5 and c7), which shifted the displacement of the warm pool from eastward to westward, appear to be the pivot point of the 1986–1989 ENSO cycle.

Following the arrival of cold SST anomaly (d8), an easterly wind anomaly developed in the western Pacific (a8) and forced an upwelling Kelvin wave (b8) that strengthened the westward displacement. The Kelvin wave reached the eastern Pacific in May 1988 (b9) and increased the regular seasonal SST cooling at its early stage (Figure 5) by raising the thermocline (Figure 3). This generated a cold SST anomaly in May–June 1988 (d9), marking the beginning of La Niña in the eastern Pacific. In the western Pacific the westward current anomaly associated with the easterly wind forcing and the upwelling Kelvin wave further developed the westward displacement of the warm pool and therefore enhanced the local cold SST anomaly (d10). Hence additional easterly wind patches developed in September 1988 (a10) which produced another upwelling Kelvin wave (b10) that propagated into the eastern Pacific (b11). This wave induced a surfacing of the thermocline (Figure 3) and so increased the seasonal SST cooling (d11). The corresponding cold SST anomaly was then advected toward the central Pacific (d12) by the westward current associated with the wave (b11). As a consequence, the easterly wind anomaly persisted in the western and central Pacific (a12), and La Niña was fully developed both in the ocean and the atmosphere.

With this schematic description in mind it is worth noting that the way SST anomalies developed over the equatorial Pacific is, to some extent, distinct during El Niño and during La Niña. During El Niño the succession of warm SST anomalies, at the South American coast, in the eastern, central, and western Pacific, resulted in an apparent westward propagation of these anomalies (Figure 8d, thick dot-dashed line) in 1987. Such migration stemmed from the different timing of two distinct SST warming periods: in February–March, the seasonal warming in the eastern Pacific reinforced by the arrival of downwelling Kelvin waves, and several months later, the warming induced by eastward advection of the warm pool in the central western Pacific. In contrast, during La Niña the cold SST anomalies started to develop in the western Pacific with the westward displacement of the warm pool; later, upwelling Kelvin waves came out and induced near the eastern Pacific coast cold SST anomalies that were probably advected toward the central Pacific. This resulted in two distinct apparent propagation of cold SST anomalies, one eastward from the western Pacific to the central Pacific and the other westward from the coast to the central Pacific (Figure 8d, the two branches of the thick dot-dashed line) in 1988. These two branches join in the central Pacific in October–November 1988, and it results in the coldest SST observed over the studied area/period, in particular, with the surfacing of the thermocline (Figure 3). In fact, it was the coldest SST recorded over the 11-year SST time series at 0–140°W (W. Kessler, personal communication, 1994).

3.4. Waves and Seasonal Cycle

In the preceding analysis, done on data sets relative to a 2-year mean reference period, it was not possible to assess the importance of the seasonal cycle, a subject of great interest for ENSO studies [e.g., *Meehl*, 1990]. However, our analysis suggests that the seasonal cycle played a notable role in the ENSO cycle, at least in the eastern Pacific. With only 28 months of Geosat data collected during strong interannual El Niño–La Niña changes, a mean seasonal cycle in sea level and zonal current anomalies cannot be reliably derived. However, a mean seasonal cycle is conceivable based on wind-forced model results [*Busalacchi and O'Brien*, 1980; *du Penhoat et al.*, 1992; *Kubota and O'Brien*, 1992; *Kessler and McCreary*, 1993], and it can be schematized as follows. In the Kelvin mode a significant downwelling wave occurs in November–December, followed by an upwelling wave around February–April. In the $m = 1$ Rossby mode a well-defined upwelling wave appears in April–August, followed by a downwelling Rossby wave in September–December (note that the dates correspond to the passage of the waves in the central equatorial Pacific).

As compared to the mean seasonal cycle, during El Niño the November–December 1986 downwelling Kelvin wave was greatly enhanced [*du Penhoat et al.*, 1992] and apparently induced an increase of the eastern Pacific seasonal SST warming. The March–July 1987 upwelling Rossby wave was also enhanced [*du Penhoat et al.*, 1992] and contributed to the continuation of the eastward displacement of the warm pool. In August 1987 to January 1988 the downwelling Rossby wave increased and, as suggested earlier, appears to be the reason

for the shift from El Niño to La Niña. During La Niña the November–December downwelling Kelvin wave was near normal in 1987 but nonexistent in 1988. The upwelling Rossby wave was also below normal (April–July 1988); in the western Pacific the corresponding eastward current was greatly exceeded by westward currents induced by the local easterly wind anomaly and its Kelvin wave response, yielding a westward displacement of the warm pool. Most of all, the upwelling Kelvin waves were stronger than the February–April seasonal upwelling Kelvin wave and, in fact, covered most of the February 1988 to January 1989 period; these waves apparently enhanced the August–October seasonal SST cooling in the eastern Pacific.

In the eastern Pacific it seems that stronger than normal downwelling (upwelling) Kelvin waves during the 1986–1987 El Niño (1988–1989 La Niña) were important, especially in term of phase, for increasing the regular seasonal SST warming (cooling). As noted in the introduction, the eastern edge of the warm pool is subject to a very weak seasonal displacement (in fact, mostly semiannual), but its strong interannual displacement appears to be chiefly due to stronger or weaker than normal seasonal equatorial Kelvin and $m = 1$ Rossby waves. A sensitivity study, performed using the current anomaly associated only with Kelvin or $m = 1$ Rossby waves, indicates that Kelvin waves are responsible for about two thirds of the eastward (westward) El Niño (La Niña) interannual displacement. While Rossby waves are of less importance for the amplitude of this zonal interannual displacement, they appear fundamental for the timing of the reversal of zonal displacement which shifts El Niño to La Niña in the central western Pacific around September 1987 (Plate 1b).

4. Conclusions and Discussion

In spite of the seminal nature of *Gill*'s [1983] work, basin-scale observed current measurements were needed to prove undeniably that ENSO SST anomalies in the central Pacific chiefly result from anomalous displacement of the warm pool. Direct current measurements from a single TOGA-TAO mooring at 0°–165°E and from several cruises along 165°E support this advective hypothesis [*McPhaden and Picaut*, 1990]. With the recent development of satellite altimetry it is now possible to derive low-frequency geostrophic zonal surface currents which agree quite well with observed currents along the Pacific equator [*Picaut et al.*, 1990]. Using a specific and careful processing of the Geosat Exact Repeat Mission (ERM) data set over the November 1986 to February 1989 period, *Delcroix et al.* [1994] improved the reliability of altimetry-derived surface current anomalies. They further showed that zonal current anomalies in the equatorial Pacific can be interpreted mainly in terms of first-baroclinic equatorial Kelvin and $m = 1$ Rossby waves forced by wind stress anomalies.

In the present study an extensive use of the aforementioned Geosat current data set, relative to the 2-year November 1986 to October 1988 period, demonstrates that the eastward (westward) displacement of the eastern edge of the warm pool was primarily due to horizontal advection by zonal current anomalies during the 1986–1987 El Niño (1988–1989 La Niña). As a corollary, El Niño (La Niña) warm (cold) SST anomalies in the central western equatorial Pacific were the result of anomalous zonal advection. Over the almost complete El Niño–La Niña ENSO cycle covered by Geosat, the displacement of the warm pool appears as a low-frequency movement (Figure 5) resulting from high-frequency forcing, i.e., a succession of local wind forcing and its remote response in the equatorial waveguide.

A series of first-baroclinic equatorial Kelvin and $m = 1$ Rossby waves was clearly identified during the El Niño–La Niña cycle (Plates 1a and 1b) and appears fundamental for the evolution of ENSO anomalies. In the eastern Pacific the simultaneous occurrence of free-propagating downwelling (upwelling) Kelvin waves with the seasonal SST warming (cooling) appears necessary for the local development of El Niño (La Niña) SST anomaly (Plates 1a and 1d). In the central western Pacific, current anomalies associated with local wind forcing, Kelvin waves, and Rossby waves were responsible for the zonal displacement of the warm pool. Although Rossby waves were of less importance for the amplitude of the displacement, a set of $m = 1$ downwelling Rossby waves shifted the warm pool displacement from eastward to westward and therefore seems to have been the cause for El Niño to shift into La Niña during the boreal fall of 1987.

Our analysis of the wave sequence started with the strong November–December 1986 Kelvin wave (i.e., at the beginning of the Geosat ERM) at the time when El Niño was already underway [*McPhaden and Hayes*, 1990; *Delcroix et al.*, 1992]. The El Niño related SST warming, which arose in September 1986 in the central eastern Pacific, was probably related to the weakening of the easterlies in the western Pacific that began in July [*McPhaden et al.*, 1988] and set up a series of equatorial Kelvin waves [*Miller et al.*, 1988] (Figure 3). As for the fully developed 1986–1987 El Niño, observational and modeling studies show that the SST warming in the east was due to the thermocline depression in the wake of Kelvin waves excited farther west [*McPhaden and Hayes*, 1990; *Seager*, 1989]. Anomalous eastward advection, mostly due to upwelling Rossby waves, also contributed to the 1986–1987 modeled El Niño warming, but with diminishing importance from west to east [*Seager*, 1989]. These results, together with the findings of *McPhaden and Picaut* [1990] on the displacement of the warm pool, are in accord with and complement our results.

One of the puzzles of the ENSO cycle is how the coupled system made its transition from an El Niño phase to a La Niña phase. Following the conceptual ideas of *McCreary* [1983] and *Schopf and Suarez* [1988], there have been numerous arguments presented about the importance of extraequatorial and equatorial Rossby waves and their reflection on the western Pacific boundary in the oscillatory nature of ENSO [*Battisti*, 1988, 1989; *Graham and White*, 1988, 1991; *Kessler*, 1991]. The delayed action oscillator [*Suarez and Schopf*, 1988], present in the prediction model of *Cane and Zebiak* [1985], requires a succession of lowest-meridional upwelling Rossby waves and their reflection as upwelling Kelvin waves to stop the El Niño unstable phase and shift it to a La Niña phase [*Battisti*, 1988; *Wakata and Sarachik*, 1991]. In the present study, not many of the Kelvin waves depicted in Plate 1a appear to be issued from a reflection of Rossby waves (Plate 1b) on the western boundary. Over the same 1986–1989 period, *Delcroix et al.* [1994] argue that local wind forcing rather that western boundary reflection appears to be responsible for most of the Kelvin waves originating from the western Pacific. This finding is confirmed over the 1992–1993 El Niño period through a detailed analysis of TOPEX/POSEIDON sea level and TOGA–TAO dynamic height anomalies (J.-P. Boulanger and C. Menkes, Propagation and reflection of long equatorial waves in the Pacific Ocean during the 1992–1993 El Niño, submitted to

Journal of Geophysical Research, 1994). On the other hand, we found that a set of $m = 1$ downwelling Rossby waves issued from the eastern Pacific was likely responsible for the shift from El Niño to La Niña in the boreal fall of 1987. The model result of *du Penhoat et al.* [1992] suggests that reflection of Kelvin waves can generate these Rossby waves in concert with local wind forcing. However, such a single-mode model prevents downward wave propagation and likely exaggerates the importance of reflected waves in the surface layer. Hence, at this stage of our reasoning, the respective contribution of local wind forcing and reflected Kelvin wave in generating the Rossby waves cannot be determined. These downwelling Rossby waves being the turning point in the 1986–1989 ENSO cycle, further studies are needed to elucidate their generation mechanism.

The slow migration of SST anomalies in the central and eastern equatorial Pacific is also central to recent arguments on ENSO mechanisms [*Cane*, 1992; *Neelin et al.*, 1992a]. According to *Neelin* [1990, 1991], ENSO type oscillations are possible in a coupled model in which the timescale of equatorial waves is unimportant (in contrast to the delayed action oscillator). The slow modes (SST modes) in this fast-wave limit are related to the timescales of advection and large-scale coupling which induce SST changes. However, recent model results [*Latif et al.*, 1993; *Jin and Neelin*, 1993] indicate that the SST modes and wave mode (i.e., the delayed action oscillator) are probably two extreme cases of the same behavior. In any case, understanding the physics responsible for the slow eastward or westward migration of SST anomalies is necessary in the search for ENSO mechanisms [*Barnett et al.*, 1991]. In our study the slow zonal migration of SST anomalies in the central and eastern Pacific was well defined (Plate 1d and Figure 8d) and appeared distinct regarding the El Niño and La Niña phases of 1986–1989. The slow migration resulted from the delayed association of two phenomena: the zonal advection in the central western Pacific and the arrival of downwelling (upwelling) Kelvin waves into the eastern Pacific, synchronous with its seasonal SST warming (cooling). Albeit different in terms of wave dynamics, as compared to the delayed action oscillator, our results suggest that zonal advection and wave dynamics were both important for the generation and migration of ENSO SST anomalies in 1986–1989.

Our major results about warm pool displacement, wave sequence, the shift from El Niño to La Niña, and the slow SST migrations are schematically presented in Figure 8. This scheme involves sequential ocean-atmosphere coupling which appears continuously over the November 1986 to February 1989 period. It is based on the accepted assumption that in the tropics, surface wind is mostly determined by SST [*Gill*, 1980; *Zebiak*, 1982; *Kleeman*, 1991; *Barnett et al.*, 1993]. The multivariate analysis of SST, surface pressure, winds, and outgoing longwave radiation of *Wang* [1992] during the warm and cold phase of 1986–1989 is consistent with our schematic view presented in Figures 8a and 8d. In particular, the surface wind stress anomalies are situated west of SST anomalies, both for the El Niño and La Niña phases. In any case a specific coupled model study would be necessary to confirm or disprove our ocean-atmosphere interaction scheme during 1986–1989.

An El Niño event is, from time to time, immediately followed by a La Niña event (Figure 1), hence the quasi-biennial appearance of ENSO oscillations superimposed on an aperiodic fluctuation of 3–8 years [*Rasmusson et al.*, 1990; *Barnett*, 1991]. With the increasing number of observations it appears that the recent ENSO behaved differently from the composite of *Rasmusson and Carpenter* [1982]. The 1982–1983 El Niño, which started unexpectedly, is the only one in which coupled anomalies propagated from the western Pacific all the way to the eastern Pacific [e.g., *Gill and Rasmusson*, 1983]; furthermore, it was not clearly followed by a La Niña. The present work focuses on the 1986–1989 ENSO cycle, which is interesting in the sense that El Niño was immediately followed by La Niña. The last 1991–1994 El Niño persisted longer than expected, and so far, no La Niña is predicted. Modeling results of *Gill* [1983] over the 1971–1973 period, of *Philander and Seigel* [1985] over the 1982–1983 period, and of *Seager* [1989] over the 1970–1987 period suggest that horizontal advection by anomalous currents is dominant in warming SST in the central equatorial Pacific during several ENSO events. Despite the specificity of each ENSO these modeling results allow us to extend to most ENSO our major conclusion that zonal anomalous advection is largely responsible for the production of ENSO SST anomalies in the central western equatorial Pacific.

ENSO prediction will be improved if oceanic models correctly reproduce the displacement of the warm pool, and as a consequence, the zonal advection in the central equatorial Pacific. However, in many ocean models and, in particular, one used for short-term climate forecasts, zonal advection is not fundamental in creating SST anomalies. For example, in the Max-Planck-Institüt model [*Latif*, 1987], meridional advection (complemented by weak contribution of zonal advection in the west and vertical advection in the east) seems to be responsible for most of El Niño SST anomalies [*Miller et al.*, 1993; *Barnett et al.*, 1991]. Also, in the *Zebiak and Cane* [1987] model the 1982–1983 El Niño SST anomalies do not migrate eastward as far as was observed [*Miller et al.*, 1993] and appear to be dominated by vertical advection. This reduced SST migration can be due to weak eastward currents, resulting from the linear assumption in modeled currents and/or from the use of only one baroclinic mode. However, in Figure 5 the similarity between the trajectories resulting from total currents or from currents restricted to the first-baroclinic Kelvin and $m = 1$ Rossby modes clearly indicates that the first-baroclinic mode is dominant in the zonal advection of the warm pool in 1986–1989.

Finally, one must remember that all these results on the physics of ENSO related to warm pool displacements and wave sequence were obtained from the use of basin-wide zonal surface current anomalies derived from altimetry measurements over an almost complete ENSO cycle. The agreement between Geosat-derived currents and TOGA-TAO observed near-surface currents along the equator is remarkable, particularly in the western Pacific (Figure 4) and especially in view of the amount of errors remaining in the Geosat data. In addition, TOGA-TAO data provided valuable information on the change in the vertical thermal structure associated with the passage of equatorial waves, in particular, with a 185-m excursion in the 0°–140°W thermocline depth between El Niño and La Niña (Figure 3). With the unprecedented data quality of the TOPEX/POSEIDON mission [*Stewart and Lefebvre*, 1992; *Picaut et al.*, 1995] the almost fully developed TOGA-TAO array [*Hayes et al.*, 1991b; *McPhaden*, 1993], the successful TOGA-Coupled Ocean-Atmosphere Response Experiment experiment [*Webster and Lukas*, 1992], and the recent model developments [e.g., *Neelin et al.*, 1992b], we have now enough tools in hand to understand most of the physics of ENSO.

Acknowledgments. This work could not have been carried out without the Geosat GDR and the TOGA-TAO data, both distributed by the National Oceanic and Atmospheric Administration. Bob Cheney's advice on the processing of the GEOSAT data and the programming support of François Masia are appreciated. The FSU wind stress and SST data were kindly provided by Jim O'Brien and Dick Reynolds, respectively. Billy Kessler is greatly acknowledged for his detailed comments on eastern boundary reflection and on the coldest SST anomalies in October–November 1988. Discussions or comments on previous versions of this paper with the following persons are greatly appreciated: Jean-Philippe Boulanger, Tony Busalacchi, Alan Clarke, Pascale Delecluse, Gérard Eldin, Mansour Ioualalen, Mike McPhaden, Christophe Menkes, Claire Périgaud, Lew Rothstein, Pierre Rual, and Richard Seager. Support for this work, as part of the TOPEX/POSEIDON Science Working Team, was provided by the Programme National de Télédétection Spatiale.

References

Anderson, D. L. T., and J. P. McCreary, Slowly propagating disturbances in a coupled ocean-atmosphere model, *J. Atmos. Sci.*, *42*, 615–629, 1985.

Barnett, T. B., The interaction of multiple time scales in the tropical climate system, *J. Clim.*, *4*, 269–285, 1991.

Barnett, T. B., M. Latif, E. Kirk, and E. Roeckner, On ENSO physics, *J. Clim.*, *4*, 487–515, 1991.

Barnett, T. B., M. Latif, N. E. Graham, M. Flügel, S. Pazan, and W. B. White, ENSO and ENSO-related predictability, I, Prediction of equatorial Pacific sea surface temperature with a hybrid coupled ocean-atmosphere model, *J. Clim.*, *6*, 1545–1566, 1993.

Battisti, D. S., Dynamics and thermodynamics of a warming event in a coupled tropical atmosphere-ocean model, *J. Atmos. Sci.*, *45*, 2889–2919, 1988.

Battisti, D. S., On the role of off-equatorial Rossby waves during ENSO, *J. Phys. Oceanogr.*, *19*, 551–559, 1989.

Bjerknes, J., Atmospheric teleconnections from the equatorial Pacific, *Mon. Weather Rev.*, *97*, 163–172, 1969.

Bjerknes, J., Large-scale atmospheric response to the 1964–65 Pacific equatorial warming, *J. Phys. Oceanogr.*, *2*, 212–217, 1972.

Busalacchi, A. J., and J. J. O'Brien, The seasonal variability in a model of the tropical Pacific, *J. Phys. Oceanogr.*, *10*, 1929–1951, 1980.

Busalacchi, A. J., K. Takeuchi, and J. J. O'Brien, Interannual variability of the equatorial Pacific, revisited, *J. Geophys. Res.*, *88*, 7551–7562, 1983.

Busalacchi, A. J., M. J. McPhaden, and J. Picaut, Variability in equatorial Pacific sea surface topography during the verification phase of the TOPEX/POSEIDON mission, *J. Geophys. Res.*, *99*, 24,725–24,738, 1994.

Canby, T. Y., El Niño's ill wind, *Natl. Geogr.*, *165*, 145–183, 1984.

Cane, M. A., Comments on "the fast-wave limit and interannual oscillations", *J. Atmos. Sci.*, *20*, 1947–1949, 1992.

Cane, M. A., and E. S. Sarachik, Forced baroclinic ocean motions, I, The linear equatorial unbounded case, *J. Mar. Res.*, *34*, 629–665, 1976.

Cane, M. A., and E. S. Sarachik, The response of a linear baroclinic equatorial ocean to periodic forcing, *J. Mar. Res.*, *39*, 651–693, 1981.

Cane, M. A., and S. E. Zebiak, A theory for El Niño and the Southern Oscillation, *Science*, *228*, 1085–1087, 1985.

Chang, P., and S. G. H. Philander, Rossby wave packets in baroclinic mean currents, *Deep Sea Res., Part A*, *36*, 17–37, 1989.

Cheney, R. E., N. Doyle, B. C. Douglas, R. Agreen, L. Miller, E. Timmerman, and D. McAdoo, *The Complete GEOSAT Altimeter GDR Handbook*, *NOAA Manual NOS NGS7*, 79 pp., Natl. Ocean Surv., Natl. Oceanic and Atmos. Admin., Silver Spring, Md., 1991.

Delcroix, T., Seasonal and interannual variability of sea-surface temperatures in the tropical Pacific, 1969–1991, *Deep Sea Res., Part I*, *40*, 2217–2228, 1993.

Delcroix, T., J. Picaut, and G. Eldin, Equatorial Kelvin and Rossby waves evidenced in the Pacific Ocean through GEOSAT sea level and surface current anomalies, *J. Geophys. Res.*, *96*, 3249–3262, 1991.

Delcroix, T., G. Eldin, M.-H. Radenac, J. M. Toole, and E. Firing, Variations of the western equatorial Pacific Ocean, 1986–1988, *J. Geophys. Res.*, *97*, 5423–5445, 1992.

Delcroix, T., J.-P. Boulanger, F. Masia, and C. Menkes, GEOSAT-derived sea level and surface current anomalies in the equatorial Pacific, during the 1986–89 El Niño and La Niña, *J. Geophys. Res.*, *99*, 25,093–25, 107, 1994.

du Penhoat, Y., T. Delcroix, and J. Picaut, Interpretation of Kelvin/Rossby waves in the equatorial Pacific from model-GEOSAT data intercomparison during the 1986–1987 El Niño, *Oceanol. Acta*, *15*, 545–554, 1992.

Gill, A. E., Some simple solutions for the heat-induced tropical circulation, *Q. J. R. Meteorol. Soc.*, *106*, 447–462, 1980.

Gill, A. E., An estimation of sea-level and surface-current anomalies during the 1972 El Niño and consequent thermal effects, *J. Phys. Oceanogr.*, *13*, 586–606, 1983.

Gill, A. E., Elements of coupled ocean-atmosphere models for the tropics, in *Coupled Ocean-Atmosphere Models*, edited by J. C. J. Nihoul, pp. 303–327, Elsevier, New York, 1985.

Gill, A. E., and E. M. Rasmusson, The 1982–1983 climate anomaly in the equatorial Pacific, *Nature*, *305*, 229–234, 1983.

Goldenberg, S. B., and J. J. O'Brien, Time and space variability of tropical wind stress, *Mon. Weather Rev.*, *109*, 1190–1207, 1981.

Graham, N. E., and W. B. White, The El Niño cycle: A natural oscillator of the Pacific ocean-atmosphere, *Science*, *240*, 1293–1302, 1988.

Graham, N. E., and W. B. White, Comments on "On the role of off-equatorial oceanic Rossby waves during ENSO," *J. Phys. Oceanogr.*, *21*, 453–460, 1991.

Harrison, D. E., Local and remote forcing of ENSO waveguide response, *J. Phys. Oceanogr.*, *19*, 691–695, 1989.

Harrison, D. E., and A. P. Graig, Ocean model studies of upper-ocean variability at 0°, 160°W during the 1982–1983 ENSO: Local and remotely forced response, *J. Phys. Oceanogr.*, *23*, 425–451, 1993.

Harrison, D. E., and P. S. Schopf, Kelvin-wave induced anomalous advection and the onset of surface warming in El Niño events, *Mon. Weather Rev.*, *112*, 913–933, 1984.

Hayes, S. P., P. Chang, and M. J. McPhaden, Variability of the sea surface temperature in the eastern equatorial Pacific during 1986–1988, *J. Geophys. Res.*, *96*, 10,553–10,566, 1991a.

Hayes, S. P., L. J. Mangum, J. Picaut, A. Sumi, and K. Takeuchi, TOGA-TAO: A moored array for real-time measurements in the tropical Pacific Ocean, *Bull. Am. Meteorol. Soc.*, *72*, 339–347, 1991b.

Jerlov, N. G., Studies of the equatorial currents in the Pacific, *Tellus*, *5*, 308–314, 1953.

Jin, F.-F., and J. D. Neelin, Modes of interannual tropical ocean-atmosphere interaction–A unified view, I, Numerical results, *J. Atmos. Sci.*, *50*, 3477–3503, 1993.

Kessler, W. S., Can reflected extra-equatorial Rossby waves drive ENSO?, *J. Phys. Oceanogr.*, *21*, 444–452, 1991.

Kessler, W. S., and J. P. McCreary, The annual wind-driven Rossby wave in the subthermocline equatorial Pacific, *J. Phys. Oceanogr.*, *23*, 1192–1207, 1993.

Kessler, W. S., M. J. McPhaden, and K. Weikmann, Forcing of intraseasonal Kelvin waves in the equatorial Pacific, *J. Geophys. Res.*, *100*, 10,613–10,631, 1995.

Kleeman, R., A simple model of the atmospheric response to ENSO sea surface temperature anomalies, *J. Atmos. Sci.*, *48*, 3–18, 1991.

Kubota, M., and J. J. O'Brien, Seasonal variations in the upper layer thickness of the tropical Pacific Ocean model, *J. Oceanogr.*, *48*, 59–76, 1992.

Latif, M., Tropical ocean circulation experiment, *J. Phys. Oceanogr.*, *17*, 246–263, 1987.

Latif, M., A. Sterl, E. Maier-Reimer, and M. M. Junge, Climate variability in a coupled GCM, I, The tropical Pacific, *J. Clim.*, *6*, 5–21, 1993.

Lukas, R., and P. J. Webster, TOGA-COARE, Tropical Ocean-Global Atmosphere Program and Coupled Ocean-Atmosphere Response Experiment, *Oceanus*, *35*, 62–65, 1992.

McCreary, J. P., Eastern tropical ocean response to changing wind systems: With application to El Niño, *J. Phys. Oceanogr.*, *6*, 632–645, 1976.

McCreary, J. P., A model of tropical ocean-atmosphere interaction, *Mon. Weather Rev.*, *111*, 370–387, 1983.

McPhaden, M. J., TOGA-TAO and the 1991–93 ENSO event, *Oceanogr. Mag.*, *6*, 36–44, 1993.

McPhaden, M. J., and S. P. Hayes, Variability in the eastern equatorial Pacific Ocean during 1986–1988, *J. Geophys. Res.*, *95*, 13,195–13,208, 1990.

McPhaden, M. J., and J. Picaut, El Niño-Southern Oscillation displace-

ment of the western equatorial Pacific warm pool, *Science*, *250*, 1385–1388, 1990.
McPhaden, M. J., H. P. Freitag, S. P. Hayes, and B. Taft, The response of the equatorial Pacific Ocean to a westerly wind burst in May 1986, *J. Geophys. Res.*, *93*, 10,589–10,603, 1988.
Meehl, G. A., Seasonal cycle forcing of El Niño-Southern Oscillation in a global coupled ocean-atmosphere GCM, *J. Clim.*, *3*, 72–98, 1990.
Miller, A. J., T. P. Barnett, and N. C. Graham, A comparison of some tropical ocean models: Hindcast skill and El Niño evolution, *J. Phys. Oceanogr.*, *23*, 1567–1591, 1993.
Miller, L., R. E. Cheney, and B. C. Douglas, GEOSAT altimeter observations of Kelvin waves and the 1986–87 El Niño, *Science*, *239*, 52–54, 1988.
Neelin, J. D., A hybrid coupled general circulation model for El Niño studies, *J. Atmos. Sci.*, *47*, 674–693, 1990.
Neelin, J. D., The slow sea surface temperature mode and the fast-wave limit: Analytic theory for tropical interannual oscillations and experiments in a hybrid coupled model, *J. Atmos. Sci.*, *48*, 584–606, 1991.
Neelin, J. D., Z. Hao, and F.-F. Jin, Reply "Comments on the fast-wave limit and interannual oscillations," *J. Atmos. Sci.*, *20*, 1950–1953, 1992a.
Neelin, J. D., et al., Tropical air-sea interaction in general circulation models, *Clim. Dyn.*, *7*, 73–104, 1992b.
Philander, S. G. H., The response of equatorial ocean to a relaxation of the trade winds, *J. Phys. Oceanogr.*, *11*, 176–189, 1981.
Philander, S. G. H., El Niño and La Niña, *J. Atmos. Sci.*, *42*, 2652–2662, 1985.
Philander, S. G. H., and A. D. Seigel, Simulation of El Niño of 1982–83, in *Coupled Ocean-Atmosphere Models*, edited by J. C. J. Nihoul, pp. 517–541, Elsevier, New York, 1985.
Philander, S. G. H., R. C. Pacanowski, N.-C. Lau, and M. J. Nath, Simulation of ENSO with a global atmospheric GCM coupled to a high-resolution tropical Pacific Ocean GCM, *J. Clim.*, *5*, 308–329, 1992.
Picaut, J., and R. Tournier, Monitoring the 1979–1985 equatorial Pacific current transports with expendable bathythermograph, *J. Geophys. Res.*, *96*, 3263–3277, 1991.
Picaut, J., S. P. Hayes, and M. J. McPhaden, Use of the geostrophic approximation to estimate time-varying zonal currents at the equator, *J. Geophys. Res.*, *94*, 3228–3236, 1989.
Picaut, J., A. J. Busalacchi, M. J. McPhaden, and B. Camusat, Validation of the geostrophic method for estimating zonal currents at the equator from GEOSAT altimeter data, *J. Geophys. Res.*, *95*, 3015–3024, 1990.
Picaut, J., A. J. Busalacchi, M. J. McPhaden, L. Gourdeau, F. I. Gonzalez, and E. C. Hackert, Open-ocean validation of TOPEX/POSEIDON sea level in the western Pacific, *J. Geophys. Res.*, in press, 1995.
Rasmusson, E. M., and T. H. Carpenter, Variations in tropical sea surface temperature and surface wind fields associated with the Southern Oscillation/El Niño, *Mon. Weather Rev.*, *110*, 354–384, 1982.
Rasmusson, E. M., X. Wang, and C. F. Ropelewski, The biennial component of ENSO variability, *J. Mar. Syst.*, *1*, 71–96, 1990.
Reynolds, R. W., A real-time global sea surface temperature analysis, *J. Clim.*, *1*, 75–86, 1988.
Rothstein, L. M., M. J. McPhaden, and J. A. Proehl, Wind-forced wave mean flow interactions in the equatorial wave guide, I, The Kelvin wave, *J. Phys. Oceanogr.*, *18*, 1435–1447, 1988.
Schopf, P. S., and M. J. Suarez, Vacillations in a coupled ocean-atmosphere model, *J. Atmos. Sci.*, *45*, 549–566, 1988.
Seager, R., Modeling tropical sea surface temperature: 1970–87, *J. Phys. Oceanogr.*, *19*, 419–434, 1989.
Stewart, R. H., and M. Lefebvre, TOPEX/POSEIDON: A contribution to the World Climate Research Program, in Aerospace Century XXI, *Adv. Astronaut. Sci.*, *64*, 117–128, 1992.
Suarez, M. J., and P. S. Schopf, A delayed action oscillator for ENSO, *J. Atmos. Sci.*, *45*, 3283–3287, 1988.
Wakata, Y., and E. S. Sarachik, On the role of equatorial ocean modes in the ENSO cycle, *J. Phys. Oceanogr.*, *21*, 434–443, 1991.
Wang, B., The vertical structure and development of the ENSO anomaly mode during 1979–1989, *J. Atmos. Sci.*, *49*, 698–712, 1992.
Webster, P. J., and R. Lukas, TOGA-COARE: The Coupled Ocean-Atmosphere Response Experiment, *Bull. Am. Meteorol. Soc.*, *73*, 1377–1416, 1992.
Wyrtki, K., El Niño—The dynamic response of the equatorial Pacific Ocean to atmospheric forcing, *J. Phys. Oceanogr.*, *5*, 572–584, 1975.
Zebiak, S. E., A simple atmospheric model of relevance to El Niño, *J. Atmos. Sci.*, *39*, 2017–2027, 1982.
Zebiak, S. E., and M. A. Cane, A model of El Niño-Southern Oscillation, *Mon. Weather Rev.*, *115*, 2262–2278, 1987.

T. Delcroix and J. Picaut, Groupe SURTROPAC, ORSTOM, BP A5, 98848, Nouméa Cedex, New Caledonia. (e-mail: picaut@noumea.orstom.nc)

(Received June 28, 1994; revised December 29, 1994; accepted April 28, 1995.)